APPLICATION OF KRIGING-BASED OPTIMIZATION AND SMOOTHED PARTICLE HYDRODYNAMICS IN DEVELOPMENT OF A MICROCHANNEL HEAT EXCHANGER MODEL

J. McLellan[1], T. Kaya[1], and J. Goldak[1]
[1]Carleton University, Ottawa, ON, Canada
joshuamclellan@cmail.carleton.ca, Tarik.Kaya@carleton.ca, jgoldak@mrco2.carleton.ca

Abstract

A microchannel heat exchanger (MCHX) is a technology that provides increased thermal efficiency in a small volume relative to other types of heat exchangers via an extremely high surface area-to-volume ratio. This characteristic is specifically valued when considering use in small modular reactors. With relatively little design information for commercial MCHXs available in open literature, development of a robust model and optimization thereof for use in nuclear reactors takes on significant importance. Some applications of this technology involve phase change, which is a challenging modelling problem given large volumetric changes of the liquid and gas phases, as well as moving boundaries at the phase interface. This problem is mitigated by use of a Lagrangian formulation such as smoothed particle hydrodynamics (SPH), whose use in the development of the MCHX model is discussed. Additionally, the Kriging optimization algorithm is introduced, includingits use to generate a suitable MCHX design.

1. Introduction

Today, a consortium of countries across the globe, including Canada, is working on designs for the next generation of nuclear reactors (Gen IV). Current reactor designs utilize components that offer opportunities for improvement, which can manifest as increases in overall performance of the plant or a reduction in capital costs associated with the construction of the plant. One technology that has the potential to provide such improvements is the microchannel heat exchanger (MCHX), a form of compact heat exchanger. While shell-and-tube heat exchangers (STHEs) are commonly used for the bulk of heat transfer applications, an MCHX could be a suitable candidate to replace a STHE given itsexcellent heat transfer characteristics and relatively simple manufacturing.

Development of this compact heat exchanger technology began with the initial efforts of Tuckerman and Pease in 1981 "on the cooling of very large-scale integrated circuits," who proposed that use of laminar flow in microchannels can lead to a large increase in the heat transferred [1]. Their work prompted research in a new field of study for electronics cooling using heat sinks with channels smaller than 200 μm. Since then, MCHXs have been used primarily in the electronics industry, in "applications where fluxes exceed 100 W/cm^2, such as high-powered microelectronics, diode array lasers, supercomputers and plasma-facing components [2]." Similar advancement of the technology occurred in parallel in the processing industry beginning with development of the printed circuit heat exchanger (PCHE), another form of compact heat exchanger, in 1980 at the University of Sydney for refrigeration applications [3,4]. Heatric Ltd. capitalized on these advancements and commercialized the technology in the mid-1980s, and has since become the leading manufacturer and developer of MCHXs.

The MCHXs created for use in the process industry today commonly use channels that are exceptionally small, having hydraulic diameters on the order of 1 to 3 mm [5]. Despite these dimensions not technically being “micro” scale, the heat exchanger retains the moniker “microchannel” given similarities in manufacturing, design, and the heat transfer principles that were initially used in designing the MCHXs for the electronics industry. These heat exchangers (HXs) are usually fabricated by first taking a plate of a desired material and chemically etching channels into its face. A large number of these etched plates are then pressed together and heated to just below the melting temperature of the material to encourage grain growth across their interfaces, producing a monolithic piece that has the same mechanical properties as the parent material via diffusion bonding [6]. The resulting compact HX has a much larger range of operating conditions compared to other types of HXs, which is generalized in Figure 1:

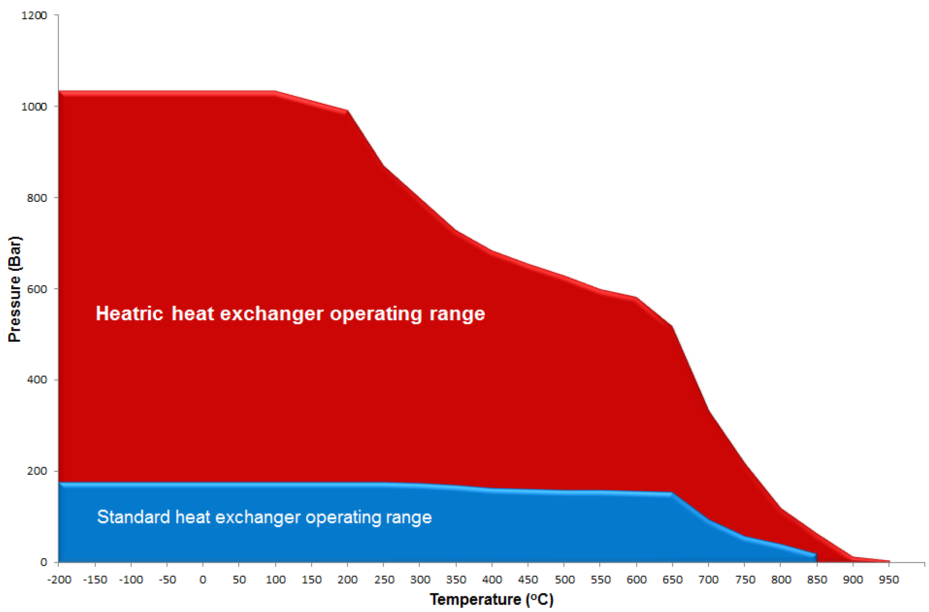

Figure 1 Temperature and pressure capabilities of the compact heat exchanger technology relative to standard HXs [7].

In addition to the excellent mechanical properties obtained, the diffusion bonding process allows for the creation of a MCHX that has an exceptionally high number of small channels that is capable of transferring higher amounts of heat than a traditional STHE due to a large surface area-to-volume ratio for the channels, while reducing the total volume of exchanger required for an equivalent heat load. The ability of the MCHX to provide excellent heat transfer and operating range in a relatively small package with ease in manufacturing is a leading motive for attempting to use it in the Gen IV designs, and possibly other compact reactor designs. This is emphasized in Figure 2 when a comparison of the relative sizes of a STHE and an MCHX designed for an equivalent heat load and input conditions are observed. A micrograph of a pair of etched plates that have been diffusion bonded is also depicted to provide a better sense of the size of the channels. While the potential of this technology for use in reactor designs has been previously noted ([8,9,10]), the relatively new nature of the MCHX technology and the lack of implementation in current reactor designs necessitates detailed analysis to generate confidence in

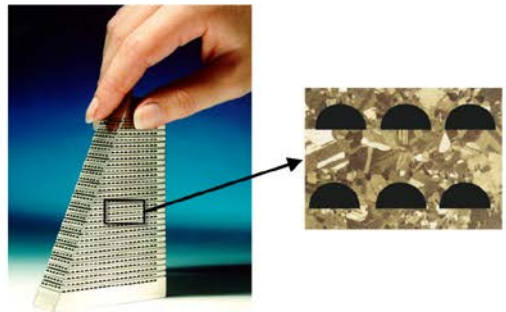

Figure 2 A STHE and equivalent MCHX (left), and sample MCHX segment with enlarged micrograph of the stacked plates (right) (Courtesy of Heatric, Ltd.).

its suitability for the proposed applications. This work introduces a new method that can be used to perform this analysis, smoothed particle hydrodynamics (SPH), chosen to augment existing finite element analysis (FEA) by virtue of its ability to treat more complex multi-phase flows with relative ease. Optimization of the MCHX technology should also be performed; a methodology for doing so is also outlined.

2. MCHX Modelling

This section details some of the MCHX modelling that has been performed to date, focusing only on the highlights of the FEA and SPH results. All models were produced using the VrSuite software package developed by Goldak Technologies Inc©, which is designed to solve coupled, transient problems in three spatial dimensions [11]. For more complete coverage of the supporting analyses and solver descriptions, please refer to the authors' previous work [2].

2.1 MCHX quarter channel FEA model

To form a basis upon which an optimization of an MCHX can be performed, a simple model of an MCHX was created, consisting of a single pair channels for hot and cold fluids, utilizing a counter-flow configuration with rectangular channels. This model utilized the existing VrSuite software FEA capabilities, which use a traditional Eulerian formulation.

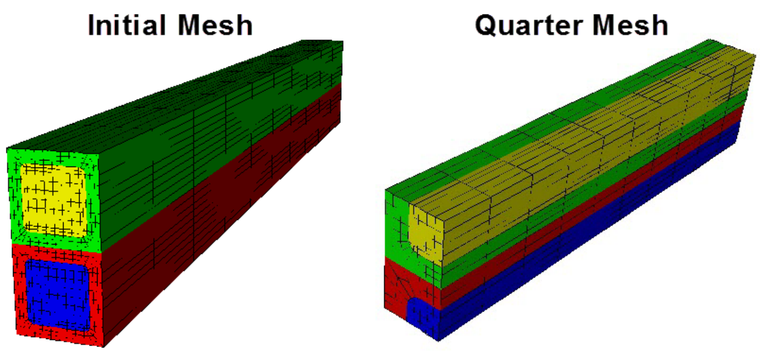

Figure 3 Initial MCHX channel pair mesh (left) and refined quarter pair mesh (right).

Use of operator splitting allows for the data to flow between three solvers: a fluid flow solver, an advection-diffusion (AD) solver, and a thermal diffusion (TD) solver. The fluid velocity profile and pressure field are first solved using the fluid flow solver without consideration of heat transfer or deformation of the solid. This data is then passed to the AD and TD solvers, which determine the temperature profiles within the fluid and solid domains respectively. The AD and TD solvers are also coupled, meaning that for any given time-step, the AD solver computes a temperature profile within the fluid first and passes the data to the TD solver to compute temperatures within the solid domain, at which point the TD solver can pass the new results back to the AD solver to use in computations for the next time step. When all boundary conditions (BCs) and initial conditions (ICs) are specified, the solvers are run concurrently to obtain a solution.

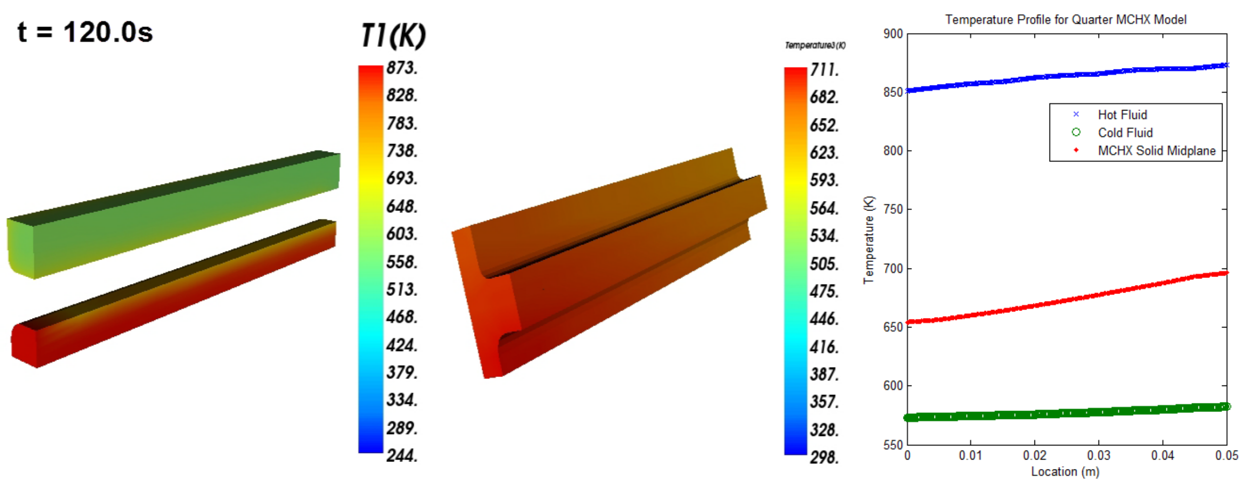

Figure 4 Fluid (left) and solid (mid) domain temperature profiles with solid mid-plane profile (right) for the quarter channel model.

The visualized temperature profiles for the fluid and solid domains are depicted on the left and middle of Figure 4 respectively. Both fluids are water with flow velocities of $v_{flow}=0.014\ m/s$, with inlet temperatures of $T_{cold}=300\ ^oC$ and $T_{hot}=600\ ^oC$. While these results are preliminary, it appears that heat is being passed from the hot channel to the cold channel through the MCHX solid as expected, a trend that is mirrored by the temperature gradients within the solid domain. High temperatures are reported near the hot fluid inlet at the bottom left of the middle image of Figure 4, and significantly colder temperatures exist near the cold fluid inlet, located at the top right of the same image. The results reported are physically realistic, enabling use of this model to form a basis for the initial optimization seen in Section 3.3.3.

2.2 Modelling with smoothed particle hydrodynamics

Typically, FEA is employed to aid in design and analysis. While traditional fixed-mesh FEA techniques have successfully been employed for initial analysis of an MCHX, attempting to apply these techniques to more complex multi-phase flows is significantly more challenging. It is possible that the operating conditions encountered by the MCHX will impose two-phase flow or boiling within the channels as fluid passes through the HX. When this occurs, there exist sharp gradients or discontinuities in the fluid properties, such as density, and moving phase boundaries that are extremely challenging to treat with the default Eulerian framework of fixed-mesh FEA. As an option to potentially overcome this issue, one can employ smoothed particle hydrodynamics, which provides a Lagrangian framework that can solve such problems with relative ease compared to the previously mentioned FEA. Instead of solving mass and heat fluxes for fixed volume elements, a domain can be modelled using a series individual particles whose "properties (e.g. temperature) [change] in accordance with a set of differential equations derived from the original governing PDEs [12]." All of the properties of interest, such as enthalpy or mass, are tracked on a per-particle basis, with momentum and heat fluxes determined by considering a region of influence around each individual particle.

The following sections detail some key SPH models created in support of the current MCHX modelling efforts. Two solvers are used for the analysis, namely the VrSuite SPH Navier-Stokes (NS) and SPH energy solvers. Fluid material properties are specified using either pressure or enthalpy alone as a primary variable for the NS and energy solvers respectively, or both for models using coupled NS and energy solvers. A more thorough outline of the SPH methodology and an initial verification of the VrSuite SPH solvers can be found in [2].

2.2.1 Free surface flows - NS

To begin developing familiarity with the SPH solvers, a simple model of a free surface flow was created utilizing only the SPH Navier-Stokes solver. A free-falling fluid "drop" is initialized at an arbitrary height above a fixed basin. The particle formations that result from the drop at different instances in time are depicted in Figure 5, starting at the top left of the image.

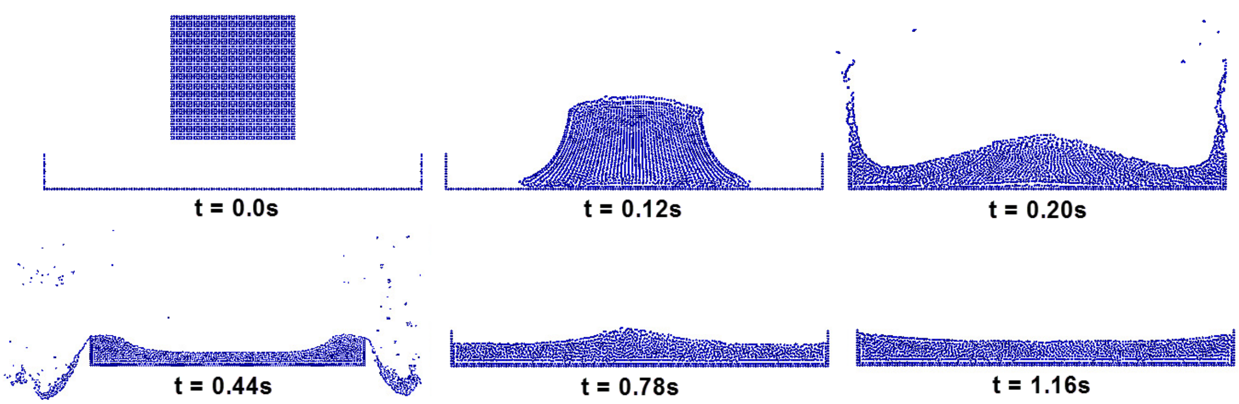

Figure 5 Temporal evolution of particle location for a free-falling liquid "drop".

After contact is made with the basin, the drop starts to deform. The particles initially located at the bottom of the drop are pushed outwards towards the side walls of the basin (top right). Upon impact with the side walls, the momentum carried by the particles causes them to jump upwards and then fall back down past the side walls (bottom left). The accumulations of particles remaining at each side of the basin generate waves that propagate back towards the centre, and subsequently back towards the side walls in an oscillatory manner. Although this analysis is primarily qualitative, this example demonstrates the ease of modelling free surface flows using SPH, and the plausible motion of the particles instils confidence that the SPH NS solver is functioning as intended. This claim is further bolstered by the agreement of this model to those performed elsewhere, such as in [13]. Additionally, this method produces comparable results for flow over a backwards-facing step, which is detailed in [2]. A more thorough assessment of the solver functionality will be performed at a later time.

2.2.2 Heat transfer and phase change– Energy

To test the SPH energy solver, a problem involving phase change via heat transfer called the Stefan problem was used. This probleminvolves a collection of SPH particles, initially in the liquid phase, having Dirichlet temperature BCs applied to both ends, while the top and bottom boundaries are treated as adiabatic. One of the Dirichlet BCs is set to below the melting temperature of the material, which causes the neighbouring particles to solidify over time. The other end is set above the melting temperature of the substance. Further details on this problem, including an analytical solution, can be found in [14].

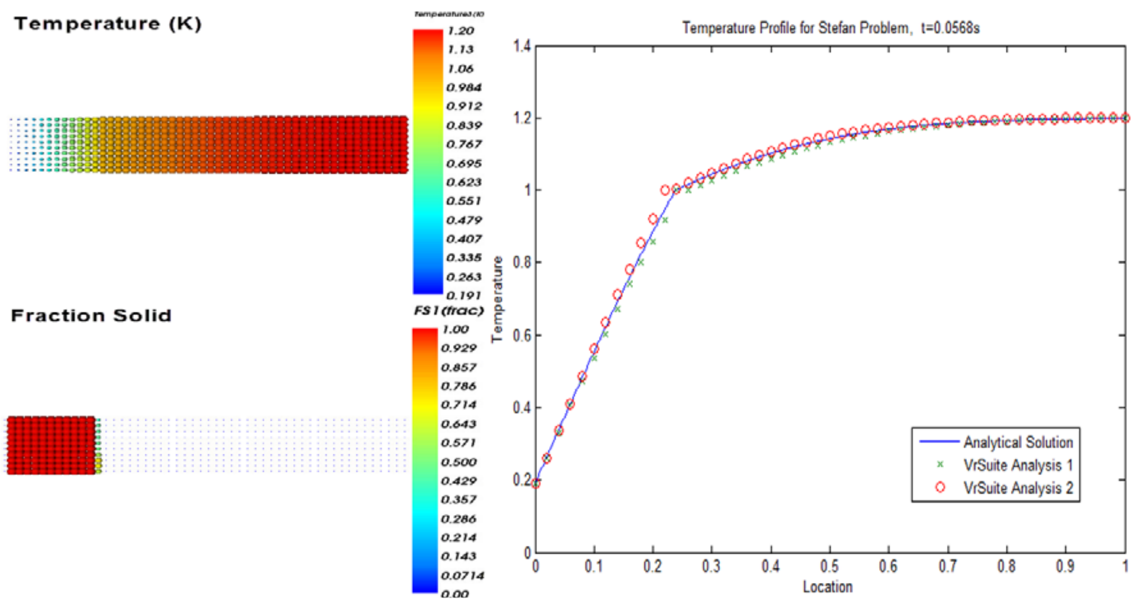

Figure 6 Visualized temperature and fraction solid (left) and corresponding solved temperature profile (right).

The temperature profile and solid fraction in the solution domain are visualized at an arbitrarily chosen time ($t=0.0568s$) in Figure 6, where a fraction solid of $FS=1.00$ indicates a particle is solid. Two independently performed VrSuite SPH analyses using the same particle discretization match the analytical solution very well, where all simulated data falls within 5.66% of the corresponding analytical value. Additionally, the simulated location of the solidification front, denoted by the location where the temperature profile “kinks”, of $x_{sim}=0.225$ compares very well with the analytically determined solution of $x_{ana}=0.2383$, differing only by 5.6%. The excellent results obtained certainly indicate that the VrSuite SPH energy solver is functional. The small discrepancies between the simulated results and the analytical solution are most likely dominated by the somewhat coarse distribution of SPH particles, which is easily overcome by increasing the number of particles. It is also worth noting that the latter problem has been extended to model phase change between liquid and vapour phases, producing equally agreeable results.

2.2.3 Boiling flows – Coupled NS and energy

Having successfully modelled free surface and heat transfer problems individually, an attempt was made to couple the two solvers to model flow boiling. As a requirement, both pressure and enthalpy must be used as primary variables to specify the water material properties. While pool boiling has been previously modelled in [2], further attempts at creating a foundation for the development of a more representative multi-channel MCHX SPH model occur in the form of a heated channel model. Here, fluid water particles enter a channel that has Dirichlet temperature BCs imposed to both sides of the channel that are much higher than the boiling temperature for water, and exits through a zero-pressure outlet at the right hand side. The flow has a Reynolds number of $Re_D = 7500$, and the features that develop are exhibited in Figure 7:

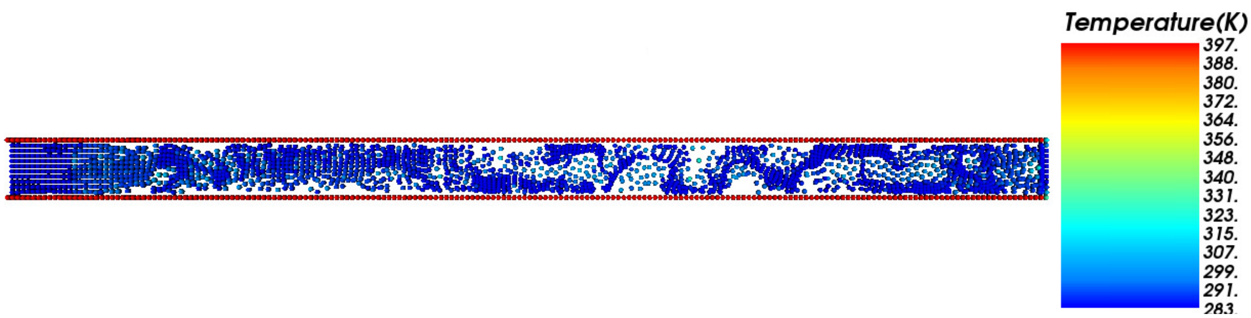

Figure 7 Boiling flow in a heated channel with inlet on the left-hand side.

The phase of the particles clearly changes from liquid to vapour during transit, evidenced by the difference in volume surrounding the light blue particles of higher temperature than the dark blue lower temperature particles entering the channel. While encouraging, these results are preliminary and only serve to demonstrate the capabilities of the SPH method and the VrSuite SPH solvers. This model will form the foundation of a more complete MCHX model consisting of a pair of channels to be created at a later date.

3. Kriging-based optimization of an MCHX

Although computational power and speed are steadily increasing, engineering analyses that are being performed for a consistently growing number of design problems continue to increase in complexity, be it through the code used or the desired level of fidelity. “In the early stages of design…, the focus is on generating, evaluating, and comparing potential conceptual configurations,” and the designer will usually attempt to achieve some measure of the impact of varying design parameters [15]. It is often impractical to use complex, full FEA or computational fluid dynamics (CFD) for these early analyses. As an alternative, metamodelling techniques can be employed, where metamodels act “as ‘surrogates’ [for] the expensive simulation process,” and can be an effective tool to aid in “design optimization, including model approximation, design space exploration, problem formulation, and solving various types of optimization problems [16].”

Development of a metamodel typically consists of choosing a method for the design of an experiment such as brute force exhaustive design or Box-Behnken, picking a model to represent the data, and then fitting the model to observed data. While there is a multitude of metamodelling techniques, a few of the more prevalent in current literature are response surface methodology, neural networks, inductive learning, and Kriging. Each method has distinct advantages. In brief, response surfaces are well suited to applications with random error, neural networks use a non-linear regression approach that can easily treat deterministic problems, and inductive learning is most useful "where the input and output factors are primarily discrete-valued or can be grouped into categories [15]."

Kriging is an interpolation method that is designed to deal with deterministic data, and offers a number of advantages over the other methods, including the ability to "provide an exact interpolation of the data or 'smooth the data'," as well as compensate for the effects of data clustering by giving less weight to points located within a cluster than individual points [15]. Additionally, Kriging models are generally more accurate for nonlinear problems, but at the expense of added complexity. Of great interest is the ability of the method to provide estimates of error and uncertainty in the value of an objective function. This allows for an algorithm to selectively choose locations within a design space to perform evaluations of a specified objective function in subsequent iterations of an optimization routine to most efficiently search for optima. These benefits form the basis for use of the Kriging method for the initial optimization of the MCHX technology seen here. For a more detailed treatment of these optimization methods, the reader is encouraged to see the works by T.W. Simpson, G.G. Wang, and S. Jeong [15, 16, 17].

3.1 General requirements for optimization

Prior to performing an optimization, the designer must first define a design space, an objective function, and any constraints that apply to the analysis. For the design space, each of *n*design variables are constrained by an upper and lower bound, and an initial set of *m* test points within these bounds are selected to create a base experimental set. Typically, this involves the creation of an *m* x *n* design of experiment (DoE) matrix, where each of the *m* rows represents an experimental analysis, and each of the columns contains design values for one of the *n* design variables of interest. An objective function must also be specified, for which a value is obtained for each analysis and serves as the key design metric for evaluating the fitness of each experimental design. After specifying any applicable design constraints, an optimization routine such as Kriging can be run to obtain a design that corresponds to an optimum value for the objective function. This usually involves minimizing or maximizing the objective function, although it is possible to also specify a target value.

3.2 Verification of the VrSuite optimization capabilities

The simple case of one-dimensional conduction in a semi-infinite bar was examined to test the functionality of the VrSuite optimization tool, using a Neumann BCof$\frac{\partial q}{\partial x}\Big|_{x=0} = 100000\ \frac{W}{m}$. The VrSuite energy equation solver was used, and the physically elapsed time was chosen as the sole design variable with a given range of *t=300s* to *t=900s*. It should be noted that the bounding values on the design variable will not necessarily be chosen as test points by the optimizer. The objective function for this test consisted of maximizing the highest temperature within the domain. For this problem, as time elapses with a prescribed heat flux applied to one end, the temperature in the domain should rise monotonically and the highest temperature within the domain should be located where the heat flux is applied. This means that to maximize the highest temperature in the problem domain, the optimization tool should return the largest elapsed time that is examined. For a more detailed examination of this test problem, including an analytical solution, please see [18].

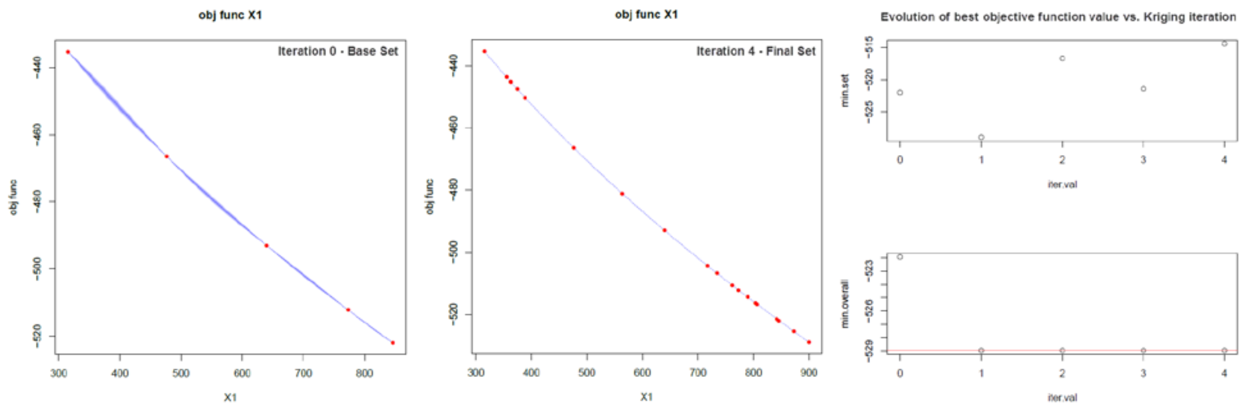

Figure 8 Objective function visualizations from optimization report created by VrSuite.

The above figure shows the evolution in the objective function values as the VrSuite optimizer runs multiple iterations, where the values of the total elapsed time are found along the abscissa and the negative value of the objective function is found along the ordinate. Note that the VrSuite optimizing tool minimizesnegative values of the objective function when maximization is chosen. As such, it is expected that longer elapsed times will yield more negative values for the objective function, which physically correspond to a higher maximum domain temperature of equal magnitude. The leftmost image contains the values for the initial set of design points chosen, which exhibit the expected trend. The blue band between points represents the uncertainty in the value of the objective function between the nodes, a visualization of the final benefit discussed in the preamble for Section 3. For subsequent iterations, the VrSuite Kriging optimizer will chose test values for the design variable to minimize this uncertainty.This is exemplified in the middle image of Figure 8, a plot of objective function values for the final iteration, where many test points where chosen at the initial locations of uncertainty. The rightmost images depict the evolution of the optimized objective function value over all Kriging iterations, with the top graph displaying the best value from each individual iteration, and the bottom graph showing the overall best value from all iterations up until the current iteration.

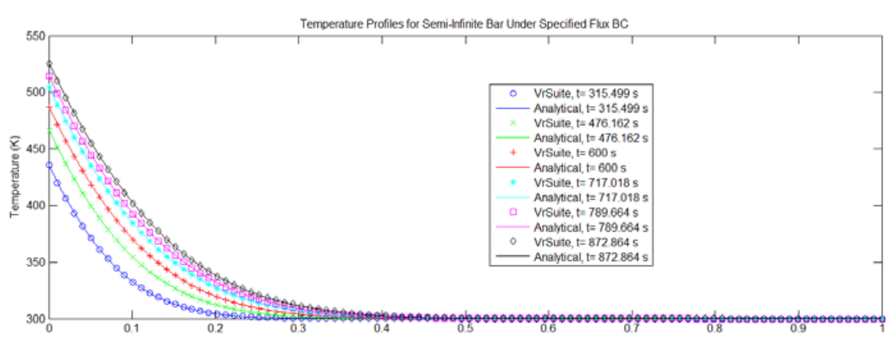

Figure 9 Domain temperature profiles for six different elapsed times for the one-dimensional semi-infinite bar with prescribed Neumann BC.

Given that the optimal value does not appear to change past the first iteration, it is likely that a sufficient number of Kriging iterations have been completed for this test analysis. Examining Figure 9, the expected trend of increasing domain temperature is reflected by the domain temperature profiles examined at some of the design variable values chosen by the VrSuite optimizing tool. The simulated values also match the analytical solution extremely closely at all times studied, and it is once again possible to claim that the semi-infinite condition is preserved given that the temperature at the end opposite where the heat flux is applied matches the initial domain temperature of $T=300K$. These results demonstrate that the VrSuite optimizer tool is functioning as intended, and that it is currently suitable to perform an initial optimization test for the MCHX technology.

3.3 Initial MCHX optimization

Before optimization of the technology can be performed, it is necessary to first create a functional base model. While it would be desirable to use a more robust SPH model that is capable of resolving more complex flow features, support for running the Kriging optimization routine with the SPH solvers has not currently been implemented in the VrSuite solver package. As such, the earlier FEM model of an MCHX channel pair, presented in Section 2.1, will be used as the basis for the initial optimization of the technology.

3.3.1 Specification of an objective function

There are varying stances on how to approach optimization of heat exchangers. Typically, an economically-driven approach is used, where the optimal design is that which provides the lowest pressure drop. This translates to the lowest operational cost given lower pumping power requirements. For this preliminary attempt at optimizing an MCHX, minimization of the pressure drop serves as a suitably simple choice of objective function. For the more detailed and representative analyses to be performed at a later date however, it is desired to use an objective function that strikes a balance between enhancement of heat transfer and reduction of frictional losses, such as that proposed in [19]:

$$F = \eta_{Nu} + \beta \eta_f \tag{1}$$

Here, η_{Nu} is a function that provides an amount of heat transfer augmentation with respect to that for a smooth surface. A similar function η_f representing the economic impact of frictional losses is also used. Finally, β is a weighting parameter that typically takes on a value between 0 and 0.1 and "accounts for the pumping cost to thermal energy cost and can be estimated using data concerning the cost of a unit of heat produced by natural fuel (e.g. natural gas) and the cost of the same amount of electric energy [19]." For the MCHX analysis, an optimal solution would be obtained through minimizing the objective function specified in Equation 1. However use of that objective function will only be fully effective once support for running optimization on problems using coupled solvers, similar to the solver coupling of the model presented in Section 2.2.3, is implemented into the VrSuite solver package, and hence will not be used until a later time. More details on the objective function suggested above can be found in [19].

3.3.2 Choice of design space

To demonstrate the capabilities of Kriging via the VrSuite optimizing tool, the design space has been limited to two variables: the channel hydraulic diameter and the inlet flow velocity.It is desired to examine the effect of altering the channel pair length and shape in future analyses. For simplicity, the hot and cold channel inlet flow speeds are constrained to be equivalent, and the overall shape of each is rectangular. The bounds on the channel size have been arbitrarily chosen given the initial nature of this analysis, but remain close to the "micro" scale dimensions of the current MCHXs that are commercially available. The lower and upper bounds for both the channel height and width have been selected to be *0.5 mm*and*5 mm*respectively. The optimizer is constrained to increment the size by no more than *1 mm*per iteration. Similarly, the flow speed bounds are somewhat arbitrary, falling between *1 m/s* and *5 m/s*, with a max increment size of *1.5 mm*. It is intended to include a larger number of design variables for future analyses, but simplicity is desired here for demonstrative purposes.

3.3.3 Initial optimum design

For the initial optimization problem, the channel is initialized with a hydraulic diameter of $D_h=3.5\ mm$, and the flow speed of both fluids is set to $v_{in}=2\ m/s$. The optimization tool is set up to use three values for each design variable in the base experimental set, and each of the three total iterations of the Kriging method subsequently utilize three new values for each variable.

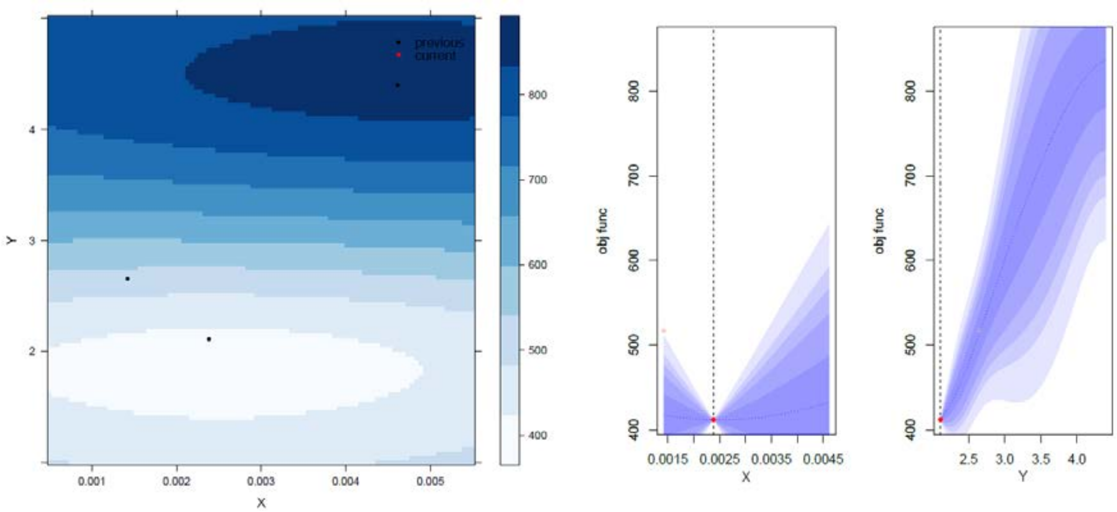

Figure 10 2-D objective function response surface (left) and corresponding value uncertainty for each design variable (right) for the first Kriging iteration.

When the optimizer is run for problems involving more than one design variable, the optimizer tool is capable of producing a 2-D response surface for the objective function, seen on the left of Figure 10, in addition to the usual plots of the uncertainty in the objective function's value versus design variable value. In this example, *X* is representative of the channel hydraulic diameter and *Y* is the inlet flow velocity. After the first Kriging iteration, the optimization tool has determined that this system has a minimum pressure drop of $\Delta p=411\ Pa$ for $D_h=2.38\ mm$ and $v_{in}=2.11\ m/s$. While changes in the hydraulic diameter appear to have a minor effect on the pressure drop, increasing the flow speed appears to be the more significant factor, which is denoted by the sharp gradients in colour in the left image of Figure 10, and is the intuitive result. These results become more refined as the optimizer continues to solve, producing an "optimal" solution where a pressure drop of $\Delta p=390\ Pa$, corresponding to$D_h=5.00\ mm$ and $v_{in}=1.00\ m/s$. This is the expected result, given by the Darcy-Weisbach equation for pressure drop, where Δp is proportional to the square of velocity, and inversely proportional to the hydraulic diameter [20]. Additionally, it is interesting to note that the design variable values designated as optimal by the solver are both bounding values. It is expected that should the range be increased, the VrSuite optimization tool would choose larger hydraulic diameter and smaller inlet flow speed values. The 2-D objective function response surface, uncertainty plot for the inlet flow speed, and convergence graph are shown below. While it appears that the optimizer has reached a converged solution, it would likely be beneficial to run the optimizer for a few more iterations.

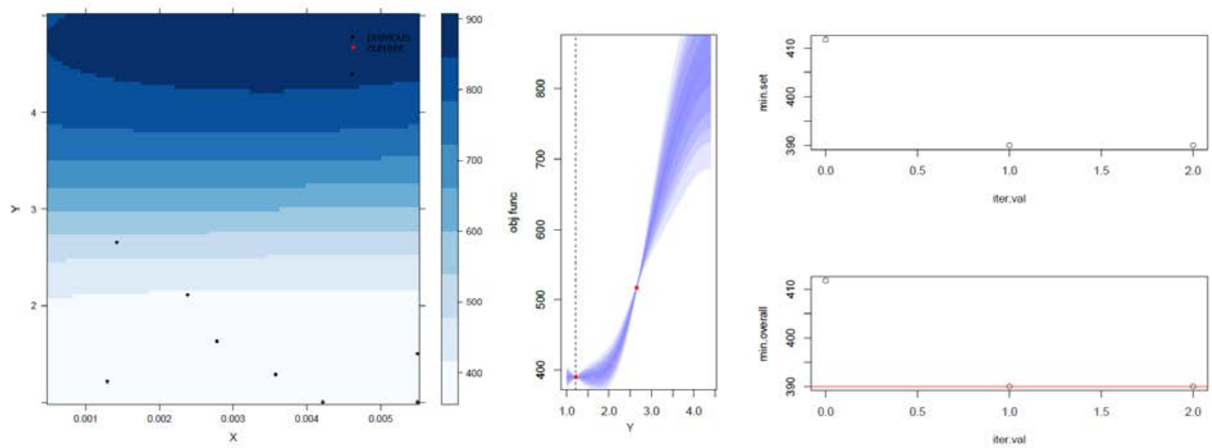

Figure 11For the last iteration, the 2-D objective function response surface (left), uncertainty plot for the inlet flow speed (mid) and optimizer convergence (right).

4. Conclusions

An initial FEM model of a MCHX channel pair was presented with results that appear realistic, and was deemed acceptable for use as the basis for an initial attempt at optimization. The SPH method was also introduced, although the models presented serve mostly validatory purposes. The free surface flow model generated using the VrSuite SPH NS solver produced seemingly realistic particle motion for a simple falling drop. Although the analysis performed has been purely qualitative, future analyses will focus on more concrete validation of the solver. Similar work was presented for the SPH energy solver, with a phase change model that showed excellent agreement between simulated and analytical results. Coupling of the NS and energy solver produced promising results for a heated channel flow model, where bubble-like features developed as a flowing fluid was heated. The Kriging methodology and an initial attempt to optimize the MCHX quarter channel pair were presented. While attempting to minimize pressure drop, the VrSuite optimization tool yielded an optimal pressure drop of $\Delta p=390\ Pa$ corresponding to the lower and upper bounds on flow speed and hydraulic diameter respectively, which was expected. While promising, it should be emphasized these results are certainly only preliminary. A more appropriate objective function and expanded design space are planned for use in later analyses.

5. Acknowledgements

The authors would like to thank Natural Resources Canada (NRCan) and the National Sciences and Engineering Research Council (NSERC) for their support of the Canadian Generation IV National Program.

6. References

[1] M. Ohadi et al. "Next generation microchannel heat exchangers", New York: Springer, 2013.

[2] J. McLellan et al. "An introduction to the use of smoothed particle hydrodynamics in the modelling and optimization of a microchannel heat exchanger", Proceedings of the 2014 Canada-China Conference on Advanced Reactor Development (CCCARD-2014), Niagara Falls, ON, Canada, 2014 Apr 27-30.

[3] D. Southall and S.J. Dewson. "Innovative compact heat exchangers", Proceedings of ICAPP '10, San Diego, CA, USA, 2010 Jun 13-17.

[4] J.E. Hesselgreaves. "Compact heat exchangers: selection, design and operations", New York: Pergamon, 2001.

[5] M.G. Khan and A. Fartaj. "A review on microchannel heat exchangers and potential applications", *International Journal of Energy Research*, Vol. 35, 2011 Jul, pp. 553-582.

[6] A. Shirzadi. "Diffusion bonding", Online Document, 2011 Nov 01 [Cited 2014 Jul 28]. Available: http://www.msm.cam.ac.uk/phase-trans/2005/Amir/bond.html.

[7] Heatric, Ltd. "The benefits of deploying Heatric exchangers: Performance", Online Document, 2014 Jul [Cited 2014 Jul 28]. Available: http://www.heatric.com/superior_performance.html.

[8] C.H. Oh et al. "Design option of heat exchanger for the next generation nuclear plant", *Journal of Engineering for Gas Turbines and Power*, Vol. 132, 2010 Mar, pp. 1-9.

[9] K. Shirvan et al. "The design of a compact integral medium size pwr", *Nuclear Engineering and Design*, Vol. 243, 2011 Nov, pp. 393-403.

[10] S. Mylavarapu et al. "Investigation of high-temperature printed circuit heat exchangers for very high temperature reactors", *Journal of Engineering for Gas Turbines and Power*, Vol. 131, 2009 Nov, pp. 1-7.

[11] Goldak Technologies Inc©. "Vr Software Suite Highlights", Online Document, 2012 Dec 06 [cited 2014 Oct 10]. Available: http://www,goldaktec.com.

[12] P.W. Cleary. "Modelling confined multi-material heat and mass flows using sph", *Applied Mathematical Modelling*, Vol. 22, 1998 Feb, pp. 981-993.

[13] J. Belin. "SPH 2d drop splash with new surface tension model and 2d shading", YouTube Video, 2013 Aug 02 [cited 2014 Aug 01]. Available: http://youtu.be/Daxzw1j7kgU.

[14] J.J. Monaghan et al. "Solidification using smoothed particle hydrodynamics", *Journal of Computational Physics*, Vol. 206, 2005 Feb, pp. 684-705.

[15] T.W. Simpson et al. "On the use of statistics in design and the implications for deterministic computer experiments", Proceedings of the 1997 ASME Design Engineering Technical Conferences, Sacramento, CA, USA, 1997 Sept 14-17.

[16] G.G. Wang and S. Shan. "Review of metamodeling techniques in support of engineering design optimization", *Journal of Mechanical Design*, Vol. 4, 2006 May 04, pp. 370-380.

[17] S. Jeong et al. "Efficient optimization design method using Kriging model", *Journal of Aircraft*, Vol. 42, 2005 Mar, pp. 413-420.

[18] T.L. Bergman et al. Fundamentals of Heat and Mass Transfer, John Wiley & Sons, Hoboken, NJ, USA, 7th edition, 2011.

[19] A.G. Kanaris et al. "Optimal design of a plate heat exchanger with undulated surfaces", *International Journal of Thermal Sciences*, Vol. 48, 2008 Nov, pp. 1184-1195.

[20] N. Ghazi and J.M. Race."Techno-economic modelling and analysis of CO_2 pipelines", *Journal of Pipeline Engineering*, Vol. 12, 2013 Jun, pp. 83-92.